ChemPhysChem

Research Article
doi.org/10.1002/cphc.202300604

Chemistry Europe
European Chemical Societies Publishing

www.chemphyschem.org

Thermal Equation of State of Cubic Silicon Carbide at High Pressures

Artem Chanyshev,*[a] Naira Martirosyan,[a] Lin Wang,[a] Amrita Chakraborti,[a] Narangoo Purevjav,[a] Fei Wang,[a] Eun Jeong Kim,[a] Hu Tang,[a] Timofey Fedotenko,[b] Shrikant Bhat,[b] Robert Farla,[b] and Tomoo Katsura[a]

We have performed in situ X-ray diffraction measurements of cubic silicon carbide (SiC) with a zinc-blende crystal structure (B3) at high pressures and temperatures using multi-anvil apparatus. The ambient volume inferred from the compression curves is smaller than that of the starting material. Using the 3rd-order Birch-Murnaghan equation of state and the Mie-Grüneisen-Debye model, we have determined the thermoelastic parameters of the B3-SiC to be $K_0 = 228 \pm 3$ GPa, $K_0' = 4.4 \pm 0.4$, $q = 0.27 \pm 0.37$, where K_0, K_0' and q are the isothermal bulk modulus, its pressure derivative and logarithmic volume dependence of the Grüneisen parameter, respectively. Using the 3rd-order Birch-Murnaghan EOS with the thermal expansion coefficient, the thermoelastic parameters have been found as $K_0 = 221 \pm 3$ GPa, $K_0' = 5.2 \pm 0.4$, $\alpha_0 = 0.90 \pm 0.02 \cdot 10^{-5} \cdot K^{-1}$, where α_0 is the thermal expansion coefficient at room pressure and temperature. We have determined that paired B3-SiC – MgO calibrants can be used to estimate pressure and temperature simultaneously in ultrahigh-pressure experiments up to 60 GPa.

1. Introduction

Silicon carbide SiC is a high hardness compound at ambient conditions. SiC has a wide range of industrial applications due to its unique properties and low cost of production. Moreover, SiC is used to modify properties of other materials via the formation of composite materials, such as diamond/SiC[1,2] carbon nanotubes/SiC.[2,3] Due to high hardness and abrasive resistance, SiC and SiC-based materials are used as abrasive materials, cutting tools, and drilling bits in manufacturing.[4] These materials are exposed to extreme conditions, and therefore it is vital to investigate SiC properties at high pressures and high temperatures.

The natural SiC is termed moissanite and it is not a common mineral, although there are rare findings on the Earth.[5–14] However, SiC may be the dominant phase in the deep interiors of carbon-rich extrasolar terrestrial planets,[15,16] and therefore control the structure and dynamics of these planets. Hence, the high-pressure investigation of SiC is important for planetary science.

SiC has a large number of polymorphs.[17] At high pressures, a polytype with a zinc-blende structure (B3) is the most studied.[18] A pioneering experimental study showed that at room temperature, it transforms into a high-pressure modification with a rock-salt structure (B1) at a pressure of about 100 GPa.[19] However, recent experimental and computational studies revealed that this transition occurs between 60 and 80 GPa at room temperature.[20–23] At high temperatures, the transition occurs at nearly the same pressures as determined at room temperature, leading to an almost zero Clapeyron slope (dP/dT).[23]

The pressure-volume equation of state (EOS) of the B3-SiC was investigated by Raman[24,25] and Brillouin[26] spectroscopies, as well as by in situ X-ray diffraction (XRD).[23,27] Thermal EOS of the B3-SiC was determined up to 60 GPa and 3300 K using laser-heated diamond-anvil cell (DAC)[23,27] and up to 8.1 GPa and 1100 K using multi-anvil apparatus.[28] However, the temperatures in the laser-heated DAC experiments fluctuate by more than ±100 K which leads to pressure fluctuations of ±1–2 GPa. Therefore, obtained EOS using laser-heated diamond-anvil cell experimental data[23,27] could be inaccurate. Multi-anvil apparatus experiments provide a much more stable temperature field with fluctuation ±5 K leading to pressure fluctuations only ±0.1–0.2 GPa. However previous experimental data were obtained in very limited pressure and temperature ranges.[28] Therefore, the thermal EOS of the B3-SiC should be re-investigated with more accurate pressure and temperature measurements over wider pressure and temperature range.

The precise determination of the EOS of the B3-SiC is valuable not only for material and planetary science but also for high-pressure technology development. In multi-anvil experiments, sample temperature is usually measured with a thermocouple, which can cause various problems. First, the thermocouple can be easily broken mechanically during sample compression. Second, it tends to be oxidised or react with cell

[a] A. Chanyshev, N. Martirosyan, L. Wang, A. Chakraborti, N. Purevjav, F. Wang, E. J. Kim, H. Tang, T. Katsura
Bayerisches Geoinstitut, University of Bayreuth, Universitätsstraße 30, 95447 Bayreuth, German
E-mail: artem.chanyshev@uni-bayreuth.de

[b] T. Fedotenko, S. Bhat, R. Farla
Deutsches Elektronen-Synchrotron DESY, Notkestr. 85, 22607 Hamburg, Germany

Supporting information for this article is available on the WWW under https://doi.org/10.1002/cphc.202300604

assembly/sample materials during heating. Third, it may cause temperature heterogeneity. Finally, thermocouple elements may contaminate the sample at high temperatures. Therefore, an alternative method to determine sample temperature without a thermocouple should be developed. One solution is to measure volumes of two standard materials with different thermal expansion coefficients by means of in situ XRD, which gives us pressure and temperature simultaneously.[29] Although this method requires synchrotron radiation, it would still be useful for the development of multi-anvil technologies, especially for ultra-high pressure generation, in which the limited space in the cell assembly makes the accommodation of a thermocouple difficult. Paired standard materials for this method should satisfy the following conditions:

1. Their thermal expansion coefficients and bulk moduli are distinctively different.
2. They do not react with each other or with surrounding materials (e.g., cell assembly materials).
3. Their crystal structures should be cubic for precise volume determination.
4. They should have high melting temperatures.

The B3-SiC – MgO pair is a good candidate for satisfying these conditions up to 60 GPa. The thermal expansion coefficient at ambient pressure and 1200 K of B3-SiC[30] and MgO[31] are 0.50×10^{-5} K^{-1} and 1.55×10^{-5} K^{-1}, respectively. Their bulk modulus coefficients are 222–228 GPa[23] and 162.8 GPa[32] for B3-SiC and MgO, respectively. Moreover, B3-SiC and MgO do not appear to form any intermediate compound, have cubic structures and have high melting temperatures, around 3100[33] and 3125 K,[33] respectively, at ambient pressure. Therefore, the thermal EOS of the B3-SiC should be carefully re-determined using reliable MgO as a pressure marker and precise thermocouple readings. The importance of carefully determining the equation of state of materials for use as pressure calibrants has been shown in plenty of studies.[34–36]

In this study, we have determined the thermal EOS of the B3-SiC using a multi-anvil apparatus in combination with in situ synchrotron XRD. We have applied our data to assess the suitability of the B3-SiC – MgO pair calibrants to simultaneously determine experimental pressures and temperatures.

Table 1. Comparison of the unit cell volumes of B3-SiC under ambient conditions

Data Source	Method	V_0, Å^3
Ref. [53]	DFT (FP-LMTO[a])	80.34
Ref. [54]	DFT (PW[b])	80.62
Ref. [55]	DFT (PPW[c])	81.97
Ref. [56]	DFT (LAPW[d])	82.88
Ref. [57]	Ab initio pseudopotential (TEP[e])	82.94
Ref. [58]	DFT (NFP[f])	81.56
Ref. [19]	Experimental (DAC)	82.92
Ref. [26]	Experimental (DAC)	82.96
Ref. [27]	Experimental (DAC)	82.80
Ref. [28]	Experimental (Multianvil)	82.85(1)

[a]Full-potential version of the linear-muffin-tin-orbital approach by Ref. [53]
[b]Pseudopotential plane-wave frozen phonon approach by Ref. [54]
[c]Pseudopotential plane-wave linear response approach by Ref. [55]
[d]Linear augmented plane-wave pseudopotential linear response approach by Ref. [56]
[e]Total-energy pseudopotential approach by Ref. [57]
[f]New full-potential linear muffin-tin orbital approach by Ref. [58]

2. Methods

The starting material was pure synthetic B3-SiC (Alfa, purity 99.8%). Reagent-grade MgO mixed with a diamond (10:1 weight %) to prevent grain growth at high temperatures was used as a pressure marker. Both sample and pressure marker were sintered at 2 GPa and 1000 K for 1 h also using the Kawai-type multi-anvil apparatus at the Bayerisches Geoinstitut, University of Bayreuth.

In situ XRD experiments were conducted using a 3×5-MN six-axis multi-anvil apparatus, Aster-15, installed at beamline P61B at the German synchrotron radiation facility, DESY.[37] This apparatus is equipped with an energy-dispersive XRD system with a Ge solid state detector (SSD) and a 4096-channel digital analyser (MCA) and with an sCMOS camera and GGG:Eu scintillator (40 um) for radiographic imaging. The incident X-rays collimated 50 μm horizontally and 250 μm vertically were directed at the sample through the gaps between the second-stage anvils. The SSD-MCA was calibrated using the γ-ray lines of ^{57}Co and ^{133}Ba at the beginning of the beam time. The diffraction angle, 2θ, was calibrated before each experiment with a precision of 0.0001°, using MgO as a standard.

Two different types of cell assemblies were used in this project. Both had boron-doped diamond (BDD) heaters but with different geometry. The first type had a strip-type BDD heater, modified from Ref. [38] This cell assembly consisted of a 7-mm $MgO+Cr_2O_3$ octahedral pressure medium, BDD heater, tetragonal MgO prism with round corners, MgO sleeve to prevent direct contact between BDD strips and $MgO+Cr_2O_3$ pressure medium, and TiC electrodes (Figure 1A). The temperature was measured using a $W_{97}Re_3$–$W_{75}Re_{25}$ thermocouple located at the centre of the furnace between the pressure marker and sample disks. The thermocouple, sample and pressure marker were isolated from the BDD stripes with the MgO prism. The second type of cell assemblies included a cylindrical BDD heater isolated from the $MgO+Cr_2O_3$ pressure medium with an MgO sleeve (Figure 1B). The temperature was also measured using a $W_{97}Re_3$–$W_{75}Re_{25}$ thermocouple located at the centre of the assembly. The sample was isolated from the BDD heater with another MgO sleeve, whereas the pressure marker was in direct contact with the heater. The thermocouple was separated from the heater with Al_2O_3 tubes. In both types of assemblies, we isolated the BDD heater from the $MgO+Cr_2O_3$ pressure medium with MgO sleeves to prevent the reduction of Cr from Cr_2O_3, since this Cr may attack the heater as well as create direct contact between the heater and thermocouple. The resistance between the heater and thermocouple was carefully monitored before and after heating to

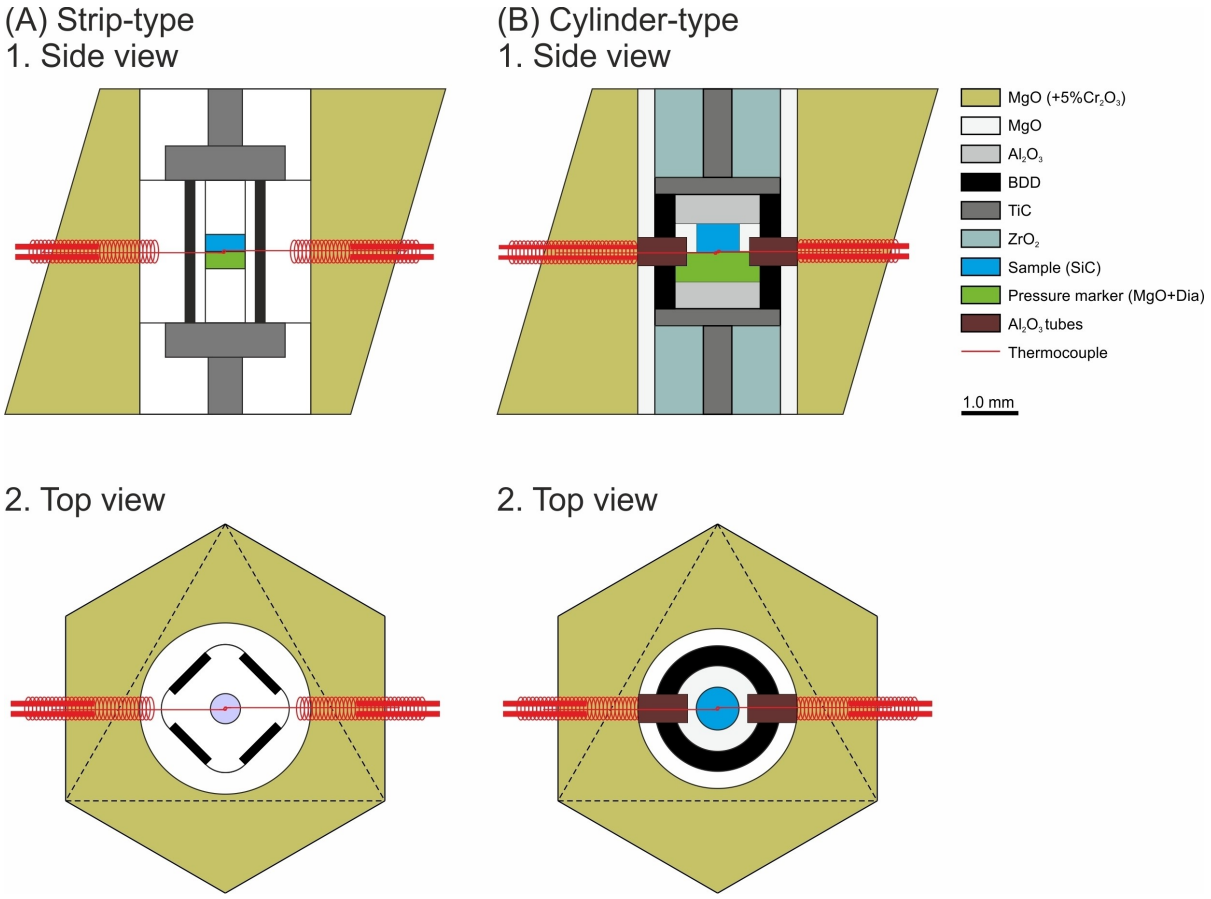

Figure 1. High-pressure cell assembly used for experiments. (A) modified cell assembly with strip-type BDD heater described in Ref. [38] (B) cell assembly with cylindrical BDD heater.

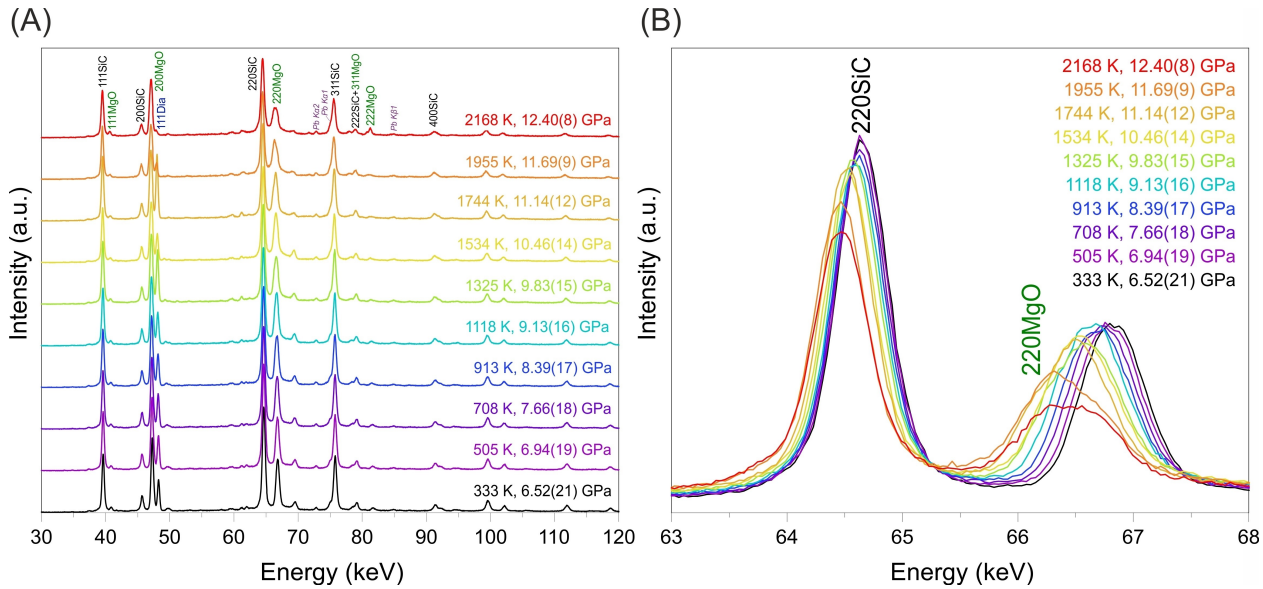

Figure 2. (A) Diffraction patterns collected during cooling from 2168 to 333 K (from 2100 to 330 K before temperature correction) at 200 bars. (B) Shifts of 220 peaks of B3-SiC and MgO during cooling from 2168 to 333 K (from 2100 to 330 K before temperature correction) at 200 bars. The numbers above the peaks indicate the Miller indices of B3-SiC (black), MgO (green) and diamond (blue). MgO peaks are from MgO sleeve and diamond peak is from BDD heater. The fluorescence lines of Pb Kα and Kβ are shown by the Siegbahn notation.

Table 2. Comparison of compressibility values for the B3-SiC fitted with the 3MB and Vinet EOS.

Data source	This work before heating without the fitting of V_0	This work after heating without the fitting of V_0	This work before heating with the fitting of V_0		Our data after heating with the fitting of V_0		Ref. [23]		Ref. [27]	Ref. [26]	Ref. [19]	Ref. [28]
EOS	3BM	3BM	3BM	Vinet	3BM	Vinet	3BM	Vinet	Vinet	3BM	3BM	BM*
V_0 (Å^3)	82.68(1)	82.68(1)	82.44(6)	82.45(6)	82.26(5)	82.26(5)	82.80	82.80	82.80	82.96	82.92	82.85(1)
K_0 (GPa)	171(3)	161(11)	190(3)	190(3)	216(6)	216(6)	224(5)	222(5)	243(5)	218(1)	260(9)	237(2)
K_0'	6.6(0.5)	11.9(2.1)	5.0(0.8)	5.1(0.8)	6.1(1.0)	6.1(1.0)	4.1(0.3)	4.3(0.4)	2.68(0.21)	3.75(0.04)	2.9(0.3)	4.0(fixed)

* Modified high-T Birch-Murnaghan EOS (truncated to third order).

confirm the reliability of the temperature measurements. The pressure effect of the thermoelectromotive force of the thermocouple was corrected using the equations determined by Ref. [39] after the experiments.

The cell assembly was compressed to the desired press load and then heated to 2100 K. After reaching this temperature, the sample was slowly cooled to 300 K with a 200-K step, collecting an XRD pattern at every step (Figure 2). In a few runs, XRD patterns were also collected during heating every 200 K. XRD patterns of the pressure marker were collected before and after the sample at a constant temperature. The accumulation times of XRD-pattern collection were 300–600 and 200–600 sec, respectively, for the sample and pressure marker. The press was oscillated around the vertical press axis between 0° and 6° during the collection to suppress intensity heterogeneities of the diffracted peaks. After cooling, the press load was decreased and the heating-cooling cycles were repeated at lower pressures. In total, 3 runs were conducted in the pressure and temperature ranges of 1.4 to 29.7 GPa and 300 to 2100 K (2213 K after the temperature correction), respectively.

The MgO and SiC diffraction peaks were fitted with a pseudo-Voigt profile function to obtain the peak positions. The defined peak positions were then used to refine the unit cell parameters using the UnitCell software.[40] The pressures were determined from the MgO unit cell volumes and pressure-corrected temperatures using the EOS proposed by Ref.[32] based on the third-order Birch–Murnaghan and Vinet EOS. The MgO unit cell volumes were calculated using seven diffraction peaks (111, 200, 220, 222, 400, 420, and 422) for precise pressure determination. B3-SiC unit cell volumes were calculated using five diffraction peaks (111, 200, 220, 311, and 400).

A 3rd-order Birch-Murnaghan[41–44] (3BM) and (b) Vinet[45,46] equations of state were used to fit the pressure-volume data at room temperature. To express the P–V–T relationship of B3-SiC, the Mie-Grüneisen-Debye[47] (MGD) and the Holland–Powell thermal pressure[48] (TP) model were used. A detailed description of the EOS models is given in supplementary materials.

3. Results and Discussion

3.1. Room temperature EOS

The unit cell volume (V_0) of B3-SiC under ambient conditions in the literature ranges from 80.34 to 82.96 Å^3 (Table 1). Our V_0 obtained by averaging several measurements under ambient conditions after experimental runs was 82.61 ± 0.01 Å^3. We used this V_0 to determine the compressibility parameters of the B3-SiC using the pressure-volume data. We fitted the data obtained before and after heating separately, since these two sets are inconsistent with each other, especially at high pressures (Figure 3). The temperatures after heating were slightly higher than 298 K due to the residual heat. The pressure-volume data before heating (cold compression data) gave the bulk modulus and its pressure derivative as $K_0 = 171 \pm 3$ GPa and $K_0' = 6.6 \pm 0.5$, respectively (Figure 3). These parameters were after heating $K_0 = 161 \pm 11$ GPa and $K_0' = 11.9 \pm 2.1$ (Figure 3). These K_0' are

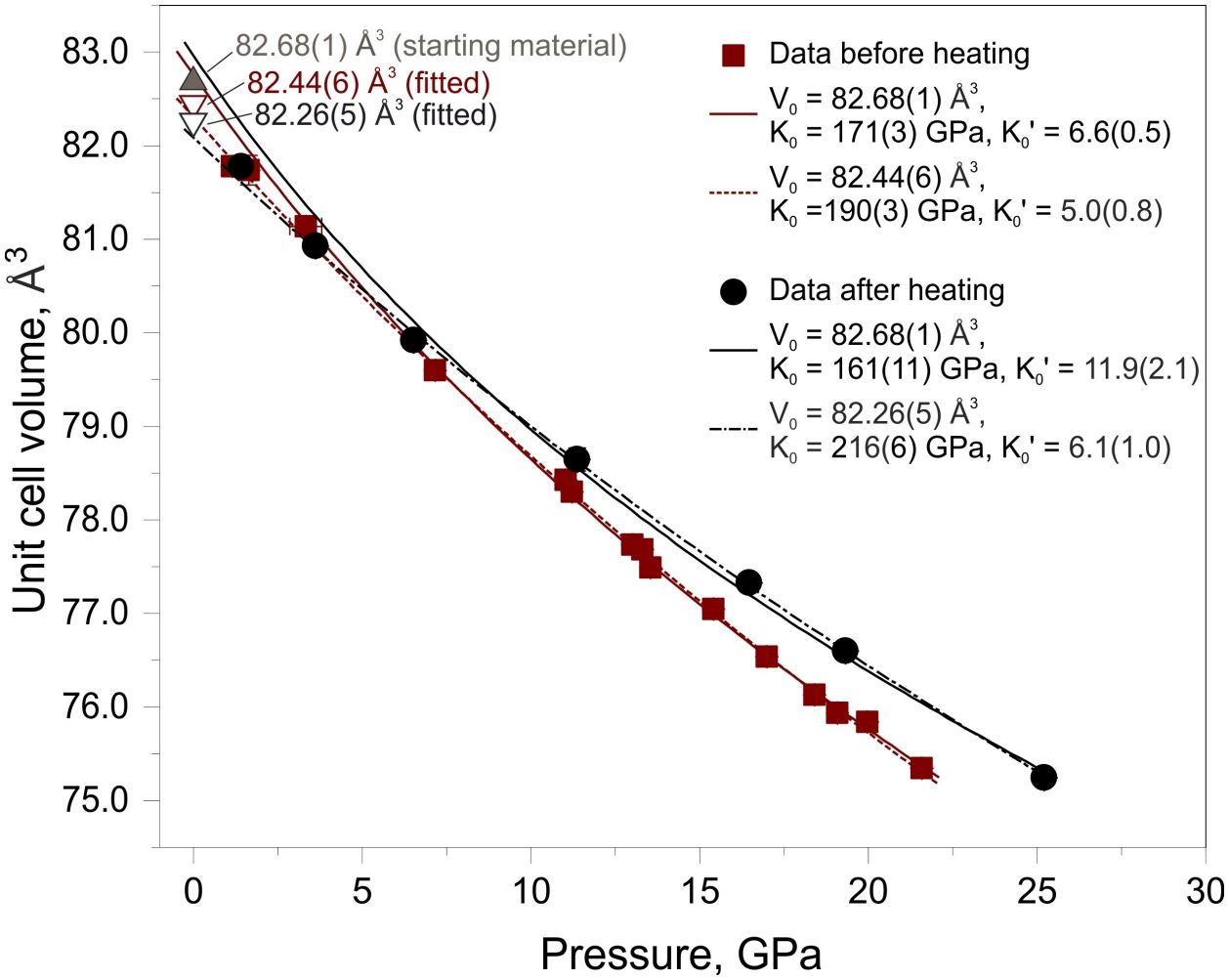

Figure 3. Comparison of the experimental data and calculated compressibility curves for data obtained before and after heating. A brown triangle indicates experimentally measured unit cell volume V_0. Data before and after heating are shown as dark red squares and black circles, respectively. Solid dark red and dotted dark red curves are compressibility curves calculated for the data obtained before heating without and with the fitting of the V_0, respectively. The open dark red triangle is fitted V_0. Thin solid black and dash-dotted black curves are compressibility curves calculated for the data obtained after heating without and with the fitting of the V_0, respectively. The open black triangle is fitted V_0.

anomalously too large, especially obtained using data after heating, and therefore V_0 was included in the fitting parameters. In this refinement, the data before heating (cold compression data) gave $V_0 = 82.44 \pm 0.06$ Å^3, $K_0 = 190 \pm 3$ GPa, and $K_0' = 5.0 \pm 0.8$ with $\chi 2 = 1.26$, where $\chi 2$ = value of the Chi-square parameter from Chi-square distribution. Those after heating yielded $V_0 = 82.26 \pm 0.05$ Å^3, $K_0 = 216 \pm 6$ GPa, and $K_0' = 6.1 \pm 1.0$ with $\chi 2 = 0.70$ (Table 2). To compare compressibility parameters from different approximations, we constructed confidence ellipses of the datasets (Figure 4).[49] We have also included data from previous studies in this figure. Calculated ellipses do not coincide with each other (Figure 4). We suppose that the low compressibility of SiC requires heating for releasing residual stresses. Therefore, we used parameters obtained only from the data after heating in the subsequent discussion. The determined bulk modulus $K_0 = 216 \pm 6$ GPa is comparable with those determined by Ref. [23,26] as 218–224 GPa. Other studies showed higher $K_0 = 237$–260 GPa.[19,27,28] Our determined $K_0' = 6.1 \pm 1.0$ is higher than those determined in previous studies.[19,23,26–28] In previous studies using DAC, *P–V* data were obtained during compression, and therefore some residual stress may remain, resulting in incorrect EOS. The refined $V_0 = 82.26 \pm 0.05$ Å^3 is smaller than that from the previous experimental studies (82.80 to 82.96 Å^3), but it is within the range of V_0 from the computational studies (80.34 to 82.94 Å^3) (Table 1).

3.2. Thermal EOS

In total, 65 data points collected during cooling from 2200 to 300 K in the pressure range 1.4–29.7 GPa were used to construct the MGD and TP models. In Table 3 the results of the fitting for both models are summarized. For the MGD model two data sets originate from fitting of *P–V–T* data using the experimentally measured unit cell volume ($V_0 = 82.61 \pm 0.01$ Å^3) and the value after fitting the room-temperature data ($V_0 = 82.26 \pm 0.05$ Å^3). The Debye temperature Θ and Grüneisen parameter γ were fixed at 1200 K and 1.06, respectively.[50,51]

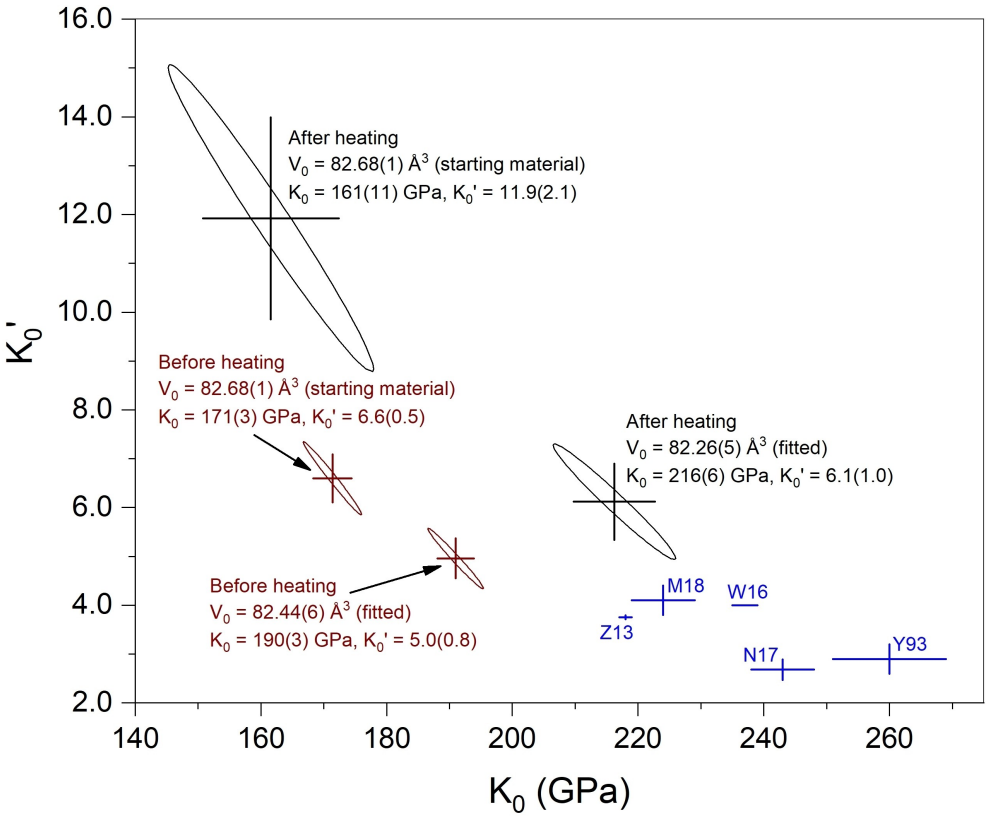

Figure 4. Comparison of compressibility values for the B3-SiC in K_0 and K_0' parameter space. For our data, confidence ellipses for a 68.3% confidence level are constructed. Data before heating are shown in brown, and data after heating are shown in black. The error bars correspond to the 1σ uncertainties on each of the individual parameters. Y93 is from Ref. [19], M18 is from Ref. [23], Z13 is from Ref. [26], N17 is from Ref. [27], W16 is from Ref. [28]

Table 3. Thermal EOS for the B3-SiC fitted with the MGD and TP models.

Data source	This work	This work	This work	Ref. [23]	Ref. [23]	Ref. [27]	Ref. [28]
EOS model	MGD	MGD	TP	MGD	TP	MGD	BM$^+$
# data points	65	65	65	105	105		26
V_0 (Å^3)	82.61(1)*	82.26(5)*	82.26(5)*	82.80	82.80	82.80	82.85(1)
K_0 (GPa)	164(5)	228(3)	221(3)	228(7)	224(2)	241, 242, 243 ± 5	237(2)
K_0'	11.5(0.9)	4.4(0.4)	5.2(0.4)	3.9(0.3)	4.1(0.14)	2.84, 2.85, 2.68 ± 0.21	4.0*
T Debye (K)	1200*	1200*		1200*		1200*	
γ0	1.06*	1.06*		1.06*		1.06*	
q	−0.12(0.55)	0.27(0.37)		−1.3(0.5)		−0.77, 0.74, 1.35 ± 0.27	
α_0 (10^{-5} K^{-1})			0.90(0.02)		0.62(0.11)	12	
T Einstein (K)			976.2*		976.2*	12	
$\alpha_T(K^{-1}) = a + bT$							
a							5.77(1)
b							1.36(2)
$(dK/dT)_P$, GPa K^{-1}							−0.037(4)
$(dK/dT)_T$, GPa^{-1} K^{-1}, 10^{-7}							−6.53(64)

* Parameters are kept fixed.
$^+$ Modified high-T Birch-Murnaghan EOS (truncated to third order).

Fitting the current data with experimentally determined $V_0 = 82.61 \pm 0.01$ Å^3 yielded $K_0 = 164 \pm 5$ GPa, $K_0' = 11.5 \pm 0.9$, and $q = -0.12 \pm 0.55$ with $\chi 2 = 4.20$, where q is the logarithmic volume dependence of γ (Figure S1, Table 3). Fitting the current data

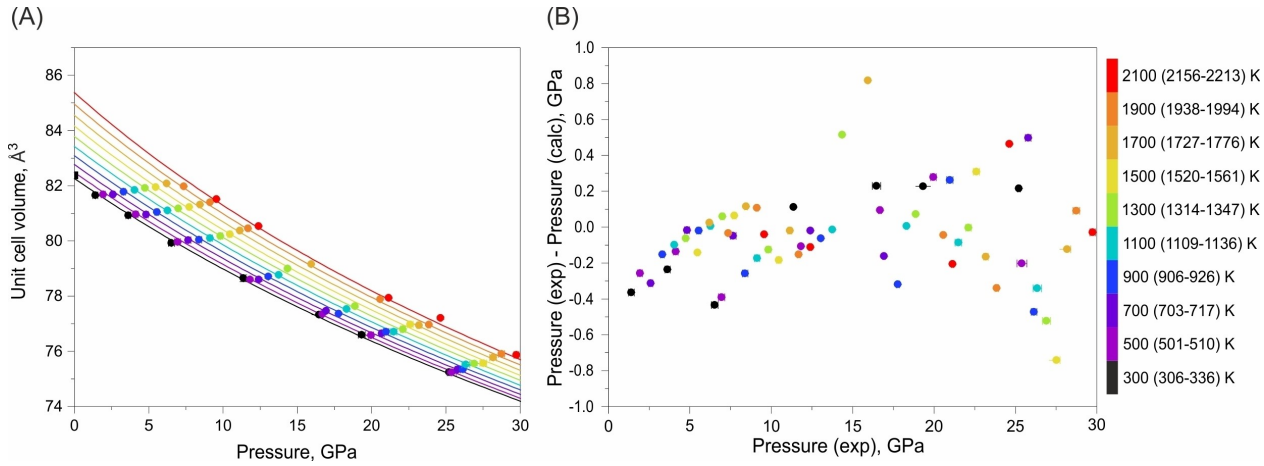

Figure 5. Results obtained fitting our data for the B3-SiC with the MGD thermal model: (A) The pressure-volume relations at elevating temperature from 306 to 2213 K. The circles are experimental data points. The curves are the results of fitting to isotherms. (B) The difference between experimental and calculated pressures at the studied pressure range. The different colors indicate different temperatures. On the right panel is the temperature scale. The numbers in the parentheses are temperatures after the pressure correction of thermocouple EMF.

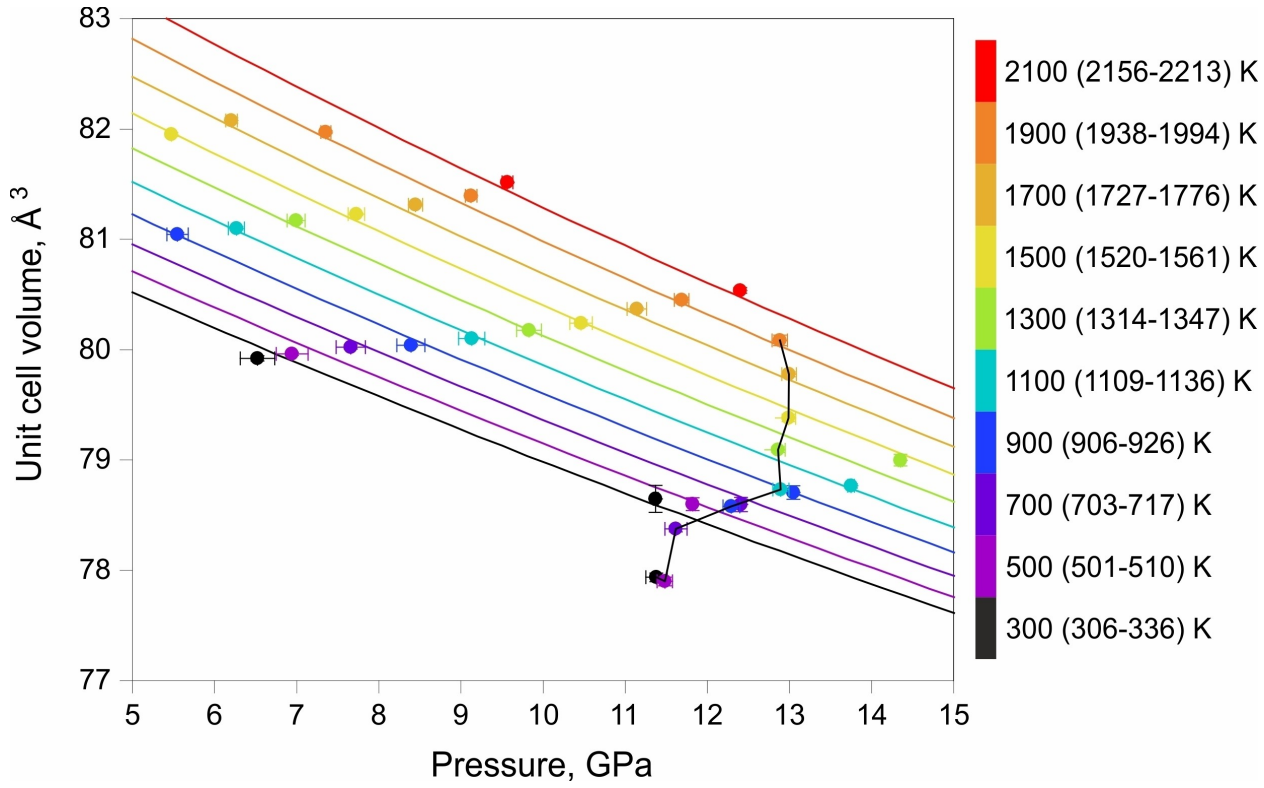

Figure 6. Comparison of heating and cooling data. The circles are experimental data points. The circles connected with a black are heating data. The curves are the results of fitting to isotherms. On the right panel is the temperature scale. The number in the parentheses are temperatures after the pressure correction of thermocouple EMF.

with the V_0 obtained after fitting the room-temperature data yielded $K_0 = 228 \pm 3$ GPa, $K_0' = 4.4 \pm 0.4$, and $q = 0.27 \pm 0.37$ with $\chi 2 = 3.33$ (Figure 5, Table 3). The $K_0 = 228 \pm 3$ GPa is comparable with that determined by Refs. [23,27,28] whereas the $K_0' = 5.3 \pm 0.4$ is higher than that determined by Refs. [23,27] (Table 3). On the other hand, our $q = 0.27 \pm 0.37$, is positive, disagreeing with Ref. [23], which gave a negative value of $q = -1.3 \pm 0.5$. A negative q may be possible, but it is unrealistic for solid materials.[52] Ref.[27] gave q between −1.25 and 0.67, depending on the selected EOS and the pressure marker. The negative value −1.25 is also unrealistic. We suppose that the thermal EOSs previously obtained by Ref. [23,27] using laser-heated DAC may contain substantial errors, probably because these studies collected the XRD data during heating, leading to the inaccurate volume parameters due to residual stress, or because

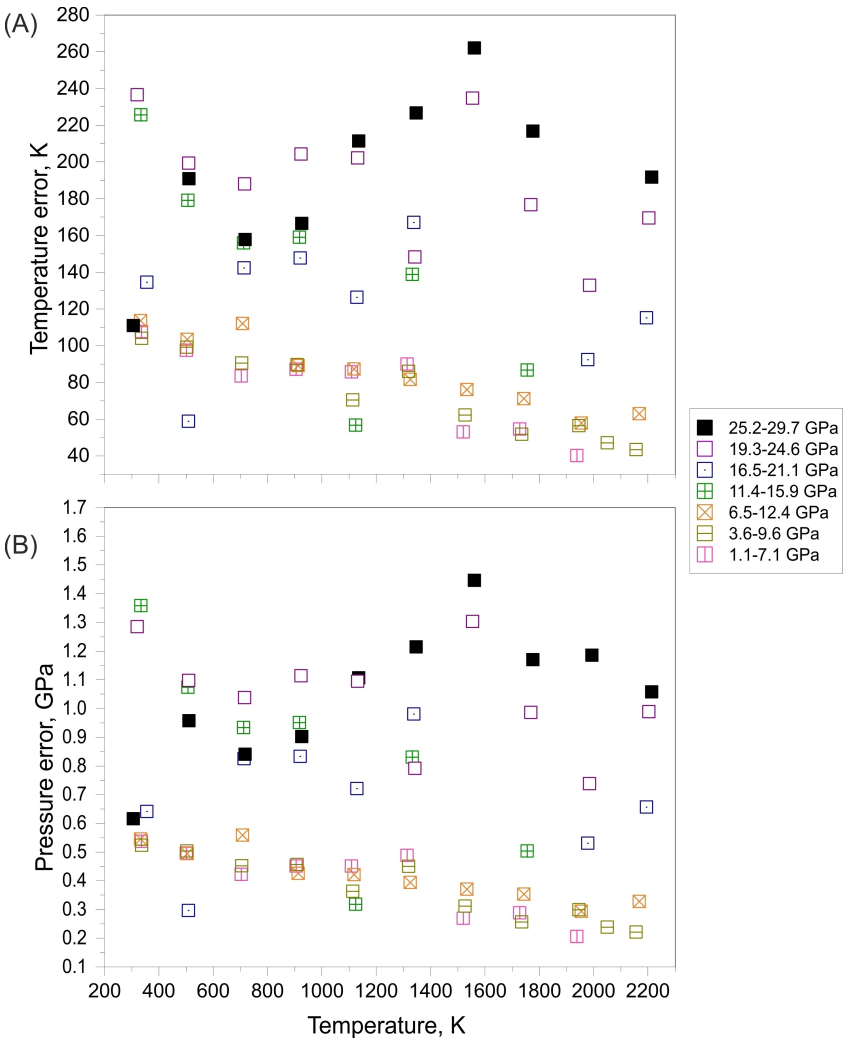

Figure 7. Temperature (A) and pressure (B) errors for data, calculated using paired B3-SiC – MgO calibrants. Different squares on the right panel show data at different pressures.

of the large uncertainties in temperature and pressure determination.

Since the pressure-volume data before and after heating are inconsistent with each other, the pressure-volume data were compared at high temperatures to find at which conditions they are consistent. The inconsistency decreased with increasing temperature, and the pressure-volume relationships became consistent above 1500 K (Figure 6). Therefore, the residual stresses should be released up to 1500 K. In a previous study performed in multi-anvil apparatus, P–V–T data were obtained only to 1100 K.[28] Therefore, their EOS (Table 3) may also contain substantial errors.

Using the 3rd-order Birch-Murnaghan EOS with the TP model, we fixed the Einstein temperature θ_E, calculated from the Debye temperature ($\theta_E = \theta_D \cdot 0.806$). This procedure yielded $K_0 = 221 \pm 3$ GPa, $K_0' = 5.2 \pm 0.4$, and $\alpha_0 = 0.90 \pm 0.02 \cdot 10^{-5} \cdot K^{-1}$ with $\chi 2 = 2.35$, where α_0 is the thermal expansion coefficient (Table 3). Among the previous experimental studies, only Ref. [23] used this model. Our bulk modulus is essentially the same as theirs, whereas their pressure derivative and the thermal expansion coefficient at ambient pressure are smaller.

3.3. Paired calibrants

The determined EOS of B3-SiC can be applied for the simultaneous pressure and temperature estimation in in situ experiments by combining it with the second calibrant of MgO. To evaluate the applicability of this method with these materials, we recalculated pressures and temperatures for each experimental point using the current 3BM + TP model for B3-SiC and 3BM + MGD model for MgO,[32] and compared them with the thermocouple temperatures and the MgO pressures based on the thermocouple temperatures (Figure S2). The observed discrepancies are within 3 GPa and 500 K. However, the majority of data points are within 1 GPa and 200 K (Figure S2). The pressure and temperature estimation uncertainties of the paired calibrant method are relatively large, up to ±1.6 GPa and ±250 K due to relatively large errors in the B3-SiC (up to

± 0.16 Å^3) and MgO (up to ± 0.14 Å^3) volumes determination in our experiments (Figure 7). In the idealized conditions, where the errors of the B3-SiC and MgO are close to 0.01 Å^3, the pressure and temperature estimation errors are much smaller, and for the experimental pressure and temperature range (1–30 GPa and 300–2200 K), the errors values are ± 0.07–0.13 GPa and ± 14–25 K. At around 60 GPa and 3000 K, assuming the similar errors for the B3-SiC and MgO volumes, the calculated pressure and temperature errors are about ± 0.17 GPa and ± 32 K. These errors are estimated as satisfactory for ultra-high-pressure experiments in multi-anvil apparatus, and therefore the B3-SiC – MgO pair could be used as paired calibrants to determine experimental pressures and temperatures simultaneously.

4. Conclusions

Polycrystalline SiC with a zinc-blende structure (B3) has been tested at high pressure and temperature using in situ synchrotron radiation. From the refinement of the XRD patterns, the unit cell volumes were obtained. Fitting the P–V–T data results in the thermal EOS of B3-SiC. Only the data obtained during cooling were adopted to build the thermal EOS due to significant residual stresses which are released only at around 1500 K. Previous studies determined the thermal EOS of B3-SiC should contain substantial errors since their P–V–T data were collected during heating or at lower temperatures. Defined compressibility parameters ($K_0 = 221 \pm 3$ GPa, $K_0' = 5.3 \pm 0.4$) are consistent with previous data, whereas the determined thermal expansion coefficient at high pressures $\alpha_0 = 0.90 \pm 0.02 \cdot 10^{-5} \cdot K^{-1}$ is 1.5 times higher than previously found. This finding enables accurate prediction of SiC's behavior at high pressures and high temperatures.

4.1. Funding Sources

This work was funded by a research project approved by the European Research Council (ERC) under the European Union's Horizon 2020 research and innovation program (Proposal No. 787 527) to T. Katsura.

Acknowledgements

We appreciate H. Fischer, S. Übelhack, R. Njul, A. Rother and U. Trenz at the Bayerisches Geoinstitut for their technical assistance. We thank G. Criniti and A. Kurnosov for helpful discussions. Open Access funding enabled and organized by Projekt DEAL.

Conflict of Interests

The authors declare no conflict of interest.

Data Availability Statement

The data that support the findings of this study are available from the corresponding author upon reasonable request.

Keywords: Silicon carbide · Equation of state · Synchrotron · Multi-anvil apparatus · High pressure

[1] J. Gubicza, T. Ungár, Y. Wang, G. Voronin, C. Pantea, T. Zerda, *Diamond Relat. Mater.* **2006**, *15*, 1452–1456.
[2] Y. Wang, T. Zerda, *J. Phys. Condens. Matter* **2007**, *19*, 356205.
[3] Y. Wang, G. Voronin, T. Zerda, A. Winiarski, *J. Phys. Condens. Matter* **2005**, *18*, 275.
[4] L. Tong, M. Mehregany, L. G. Matus, *Appl. Phys. Lett.* **1992**, *60*, 2992–2994.
[5] Q. Xuexiang, Y. Jingsui, X. Zhiqin, B. Wenji, Z. ZhongMing, F. Qingsong, *Acta Petrol. Sin.* **2007**, *23*, 3207–3214.
[6] S. Xu, W. Wu, W. Xiao, J. Yang, J. Chen, S. Ji, Y. Liu, *Mineral. Mag.* **2008**, *72*, 899–908.
[7] J. Bauer, J. Fiala, R. Hřichová, *Am. Mineral.s* **1963**, *48*, 620–634.
[8] S. Di Pierro, E. Gnos, B. H. Grobety, T. Armbruster, S. M. Bernasconi, P. Ulmer, *Am. Mineral.* **2003**, *88*, 1817–1821.
[9] Z. Zhang, J. Mao, F. Wang, F. Pirajno, *Am. Mineral.* **2006**, *91*, 1178–1183.
[10] R. B. Trumbull, J.-S. Yang, P. T. Robinson, S. Di Pierro, T. Vennemann, M. Wiedenbeck, *Lithos* **2009**, *113*, 612–620.
[11] R. Moore, J. Gurney, *Mineral inclusions in diamonds from the Monastery kimberlite*, South Africa, **1986**.
[12] M. Otter, J. Gurney, *Mineral inclusions in diamonds from the Sloan diatremes*, Colorado-Wyoming State Line kimberlite district. North America, **1986**.
[13] I. S. Leung, *Am. Mineral.* **1990**, *75*, 1110–1119.
[14] A. Gorshkov, L. Bershov, I. Ryabchikov, A. Sivtsov, M. Lapina, Y. Bao, *Geochem. Int.* **1997**, *35*, 695–703.
[15] J. C. Bond, D. P. O'Brien, D. S. Lauretta, *Astrophys. J.* **2010**, *715*, 1050.
[16] J. W. Larimer, *Geochim. Cosmochim. Acta* **1975**, *39*, 389–392.
[17] R. Cheung, *Silicon carbide microelectromechanical systems for harsh environments*, World Scientific **2006**.
[18] K. Daviau, K. K. Lee, *Crystals* **2018**, *8*, 217.
[19] M. Yoshida, A. Onodera, M. Ueno, K. Takemura, O. Shimomura, *Phys. Rev. B* **1993**, *48*, 10587.
[20] Y. Kidokoro, K. Umemoto, K. Hirose, Y. Ohishi, *Am. Mineral.* **2017**, *102*, 2230–2234.
[21] B. Thakore, S. Khambholja, A. Vahora, N. Bhatt, A. Jani, *Chin. Physics B* **2013**, *22*, 106401.
[22] K. Daviau, K. K. Lee, *Phys. Rev. B* **2017**, *95*, 134108.
[23] F. Miozzi, G. Morard, D. Antonangeli, A. N. Clark, M. Mezouar, C. Dorn, A. Rozel, G. Fiquet, *J. Geophys. Res. Planets* **2018**, *123*, 2295–2309.
[24] W. Bassett, M. Weathers, T. C. Wu, T. Holmquist, *J. Appl. Phys.* **1993**, *74*, 3824–3826.
[25] A. Debernardi, C. Ulrich, K. Syassen, M. Cardona, *Phys. Rev. B* **1999**, *59*, 6774.
[26] K. Zhuravlev, A. F. Goncharov, S. Tkachev, P. Dera, V. Prakapenka, *J. Appl. Phys.* **2013**, *113*, 113503.
[27] C. Nisr, Y. Meng, A. MacDowell, J. Yan, V. Prakapenka, S. H. Shim, *Journal of Geophysical Research: Planets* **2017**, *122*, 124–133.
[28] Y. Wang, Z. T. Liu, S. V. Khare, S. A. Collins, J. Zhang, L. Wang, Y. Zhao, *Appl. Phys. Lett.* **2016**, *108*.
[29] R. Farla, *J. Synchrotron Radiat.* **2023**, *30*.
[30] D. Talwar, J. C. Sherbondy, *Appl. Phys. Lett.* **1995**, *67*, 3301–3303.
[31] R. R. Reeber, K. Goessel, K. Wang, *Eur. J. Mineral.* **1995**, *7*, 1039–1047.
[32] Y. Tange, Y. Nishihara, T. Tsuchiya, *Journal of Geophysical Research: Solid Earth* **2009**, *114*.
[33] W. M. Haynes, D. R. Lide, T. J. Bruno, *CRC handbook of chemistry and physics*, CRC press **2016**.
[34] S. Anzellini, L. Burakovsky, R. Turnbull, E. Bandiello, D. Errandonea, *Crystals* **2021**, *11*, 452.
[35] P. I. Dorogokupets, A. Dewaele, *High Pressure Res.* **2007**, *27*, 431–446.
[36] K. Jin, Q. Wu, H. Geng, X. Li, L. Cai, X. Zhou, *High Pressure Res.* **2011**, *31*, 560–580.
[37] R. Farla, S. Bhat, S. Sonntag, A. Chanyshev, S. Ma, T. Ishii, Z. Liu, A. Néri, N. Nishiyama, G. A. Faria, *J. Synchrotron Radiat.* **2022**, *29*.
[38] K. Nishida, L. Xie, E. J. Kim, T. Katsura, *Rev. Sci. Instrum.* **2020**, *91*, 095108.

[39] Y. Nishihara, S. Doi, S. Kakizawa, Y. Higo, Y. Tange, *Phys. Earth Planet. Inter.* **2020**, *298*, 106348.
[40] T. J. B. Holland, S. A. T. Redfern, *Mineral. Mag.* **1997**, *61*, 65–77.
[41] F. D. Murnaghan, *Am. J. Math.* **1937**, *59*, 235–260.
[42] F. Birch, *Phys. Rev.* **1947**, *71*, 809.
[43] F. Birch, *J. Geophys. Res. Solid Earth* **1978**, *83*, 1257–1268.
[44] T. Katsura, Y. Tange, *Minerals* **2019**, *9*, 745.
[45] P. Vinet, J. Ferrante, J. Smith, J. Rose, *J. Phys. C* **1986**, *19*, L467.
[46] P. Vinet, J. Ferrante, J. H. Rose, J. R. Smith, *Journal of Geophysical Research: Solid Earth* **1987**, *92*, 9319–9325.
[47] J. Jamieson, J. Fritz, M. Manghnani, in *High-Pressure Research in Geophysics*, Center for Academic Publications, Tokyo **1982**, 27–48..
[48] T. Holland, R. Powell, *J. Metamorph. Geol.* **2011**, *29*, 333–383.
[49] R. J. Angel, *Rev. Mineral. Geochem.* **2006**, *41*, 35–59.
[50] J. D. Clayton, *A geometrically non-linear model of ceramic crystals with defects applied to silicon carbide (SiC)*, ARMY RESEARCH LAB ABERDEEN PROVING GROUND MD **2010**.
[51] G. A. Slack, *J. Appl. Phys.* **1964**, *35*, 3460–3466.
[52] Q. Liu, L. R. Chen, *Indian J. Pure Appl. Phys.* **2017**, *55*, 368–371.
[53] W. Lambrecht, B. Segall, M. Methfessel, M. Van Schilfgaarde, *Phys. Rev. B* **1991**, *44*, 3685.
[54] N. Churcher, K. Kunc, V. Heine, *J. Phys. C* **1986**, *19*, 4413.
[55] K. Karch, P. Pavone, W. Windl, O. Schütt, D. Strauch, *Phys. Rev. B* **1994**, *50*, 17054.
[56] C.-Z. Wang, R. Yu, H. Krakauer, *Phys. Rev. B* **1996**, *53*, 5430.
[57] K.-J. Chang, M. L. Cohen, *Phys. Rev. B* **1987**, *35*, 8196.
[58] M. Prikhodko, M. Miao, W. R. Lambrecht, *Phys. Rev. B* **2002**, *66*, 125201.

Manuscript received: August 24, 2023
Revised manuscript received: February 16, 2024
Version of record online: March 1, 2024